BIOINFORMATION
Discovery at the interface of physical and biological sciences

open access www.bioinformation.net Hypothesis

Volume 7(4)

MD simulation and experimental evidence for Mg^{2+} binding at the B site in human AP endonuclease 1

Numan Oezguen[1$*], Anil K. Mantha[2$], Tadahide Izumi[3], Catherine H. Schein[2], Sankar Mitra[2], Werner Braun[2]

[1]Internal Medicine-Endocrinology Department, University of Texas Medical Branch, Galveston, TX 77555-1060, USA; [2]Department of Biochemistry and Molecular Biology, University of Texas Medical Branch, Galveston, TX 77555-1079, USA; [3]Stanley S. Scott Cancer Center and Department of Otolaryngology, 533 Bolivar St., University Health Sciences Center, New Orleans, LA 70112, USA; $ - These authors contributed equally to this work. Numan Oezguen – Email: nuoezgue@utmb.edu; Phone: +1-409-772-2843; Fax: +1-409-772-8709; *Corresponding author

Received September 03, 2011; Accepted October 03, 2011; Published October 14, 2011

Abstract:
Apurinic/apyrimidinic endonuclease 1 (APE1), a central enzyme in the base excision repair pathway, cleaves damaged DNA in Mg^{2+} dependent reaction. Despite characterization of nine X-ray crystallographic structures of human APE1, in some cases, bound to various metal ions and substrate/product, the position of the metal ion and its stoichiometry for the cleavage reaction are still being debated. While a mutation of the active site E96Q was proposed to eliminate Mg^{2+} binding at the "A" site, we show experimentally that this mutant still requires Mg^{2+} at concentration similar to that for the wild type enzyme to cleave the AP site in DNA. Molecular dynamics simulations of the wild type APE1, E96Q and a double missense mutant E96Q + D210N indicate that Mg^{2+} placed at the A-site destabilizes the bound AP site-containing DNA. In these simulations, the H-bond chain D238-H309-AP site oxygen is broken and the substrate DNA is shifted away from its crystal structure position (1DE9). In contrast, simulations with the Mg^{2+} at site B or A+B sites leave the substrate DNA at the position shown in the crystal structure (1DE9). Taken together our MD simulations and biochemical analysis suggests that Mg^{2+} binding at the B site is involved in the reaction mechanism associated with endonuclease function of APE1.

Keywords: Ref-1, Base excision repair, DNA binding, Phosphodiester

Abbreviations: APE, AP-endonuclease; AP site, apurinic/apyrimidinic site; BER, base excision repair; Ref-1, redox factor 1; hAPE1, human APE1; WT, wild type; MD, molecular dynamics; THF, tetrahydrofuran.

Background:
DNA is constantly damaged due to intrinsic and extrinsic genotoxic agents including reactive oxygen species (ROS) and ionizing radiation. It is estimated that as many as 10^3-10^5 base lesions are endogenously induced per day in a mammalian genome **[1,2]** which include oxidized bases, single-strand breaks (SSBs) and apurinic/apyrimidinic (AP) sites. These lesions are often cytotoxic and mutagenic **[3].** Hence their repair is imperative for maintaining genome integrity. The base excision repair (BER) pathway is the primary process for repairing AP sites in which AP endonuclease (APE1) has the central role **[4].** APE1 hydrolyzes the phosphodiester backbone of the DNA 5' to the AP site and generates 3'-OH and 5'-deoxyribose phosphate (dRP) that has to be removed before gap filling repair synthesis by a DNA polymerase followed by ligation of the nick by a DNA ligase **[5].**

The structure and mechanism of APE1 has been studied extensively **[6],** and there are nine crystal structures available in the PDB-databank (**Table 1, see supplemetray material).**

Mundle *et al.* **[7]** showed that the Mg^{2+}-assisted cleavage is a one-step (concerted) reaction. One crystal structure of APE1 and product DNA (1DE9) has a single Mn^{2+} metal ion **[8]** at a position called the A site. The Mn^{2+} in this crystal structure is coordinated by the carboxyl group of E96. Five more crystal structures without substrate or product DNA have also one metal ion each (Sm^{3+}, Pb^{2+}, and Mg^{2+}) at the A site **[8-11] (Table 1, see supplemetray material).** Another crystal structure of free APE1 shows two non-catalytic metal Pb^{2+} ions at positions defined as A and B site **[10].** The B site Pb^{2+} is close to residue D210 which is essential for the endonuclease activity **[12, 13].** We showed in an earlier Molecular Dynamic (MD) simulation study the existence of two low potential energy sites for a single Mg^{2+} in pre-cleavage complexes of AP site-containing DNA substrate and APE1 **[14].** These two sites were close to the A- and B sites. In that study we also proposed the "moving metal" mechanism **[14].** It is essentially the same single Mg^{2+} ion mechanism as proposed by Mol *et al.* **[8].** The difference was the location of the Mg^{2+} in the pre-cleavage state. In the simulation study with the APE1-substrate DNA complex in the pre-cleavage state, the Mg^{2+} ion was held most stably at the B site. It then moved to the A site after cleavage of the substrate DNA. Similar mechanisms involving movement of a catalytic metal ion have been suggested for other enzymes, such as for *E. coli* ribonuclease **[15]** and restriction endonucleases **[16].** On the other hand, cleavage reaction with two metal ions proposed by Beernink *et al.* **[10]** assumes that the site B metal activates a coordinating water molecule to produce the OH^- for the nucleophilic attack. The second metal at the site A would then stabilize the leaving 3′ end of the product.

In a recent solid state NMR study of APE1 the authors observed in the first part (APE1 without the substrate DNA) two Mg^{2+} ion signals **[17].** They also found in the second part (in the presence of substrate DNA) of that study that both the E96Q mutant (an A-site mutant) and the double mutant E96Q/D210N had equivalent Mg^{2+} binding, i.e. the difference spectrum for these two mutants was null. Their interpretation of this was that neither mutant was capable of binding Mg^{2+}, and that there was no second binding site (B site) for Mg^{2+} in the active site. In the present study, we have confirmed that, as with the E96A mutant we had examined previously **[18],** had endonuclease activity in presence of Mg^{2+}. To explore the nature of the binding sites, we carried out MD simulations with Mg^{2+} ion(s) placed at the A-, B or A+ B sites in pre-cleavage substrate DNA complexes of WT APE1, and its E96Q and E96Q/D210N (named ED) mutants. These simulations showed that Mg^{2+} at the A-site destabilizes the substrate DNA, while Mg^{2+} at B or A+B site leaves the substrate DNA at the position observed in the crystal structure (1DE8) of Mol *et al.* **[8].**

Methodology:

***Construction of WT and E96Q Mutant APE1 Polypeptides*:**

The coding sequence for full-length human APE1 was inserted in the pET15b vector (Novagen) at NdeI/XhoI sites for expression of APE1 in *E. coli*. The source of the WT APE1 cDNA was described earlier **[19].** The point mutation at residue 96 from glutamic acid to glutamine (E96Q) we created by using a site-directed mutagenesis kit and following the manufacturer's guidelines (QuickChange II XL, Agilent Technologies, Santa Clara, CA, USA). Briefly, APE1 cDNA was used as the template in PCR for generating the E96Q mutation with forward (5' ccagatatactgtgccttcaacagaccaaatgttcagag 3') and reverse (3' ggtctatatgacacggaagttgtctggtttacaagtctc 5') primers that were designed with the help of "The QuikChange® Primer Design Program" (available at http://www.genomics.agilent.com). The DNA sequences of the WT and mutant E96Q APE1 cDNA were confirmed in UTMB's Recombinant DNA Laboratory (RDL).

Expression and Purification of WT APE1 and E96Q Polypeptides:

The WT APE1 and E96Q mutant proteins were purified as previously described **[18, 20]** with slight modifications. The proteins possessing a C-terminal His6-tag were purified via immobilized metal affinity and ion-exchange chromatography. Briefly, the *E. coli* BL21 (DE3)/RIPL cells were transformed with the pET15b-derivatives and the bacterial culture (1L in LB broth) were grown to an OD600 of 0.6. Then the APE1 protein was induced with 0.5 mM isopropyl-ß-D-thiogalactopyranoside (IPTG) at 16 ^oC for 14-16 h. The cells were then resuspended in a lysis/binding buffer containing 20 mM Tris-HCl (pH 8.0) and 0.5 M NaCl, sonicated and centrifuged. The supernatants were loaded on a 3 ml column of Ni-NTA (Qiagen). After washing the column with 18 ml lysis/binding buffer and then with the same buffer containing 20 mM imidazole, the proteins were eluted with 10 ml lysis buffer containing 200 mM imidazole, and dialyzed against 20 mM Tris-Cl (pH 8.0), 100 mM NaCl, 1 mM EDTA, 1 mM dithiotreitol (DTT) and 10% glycerol. The histidine tag was removed from the proteins after overnight incubation (16 h) with thrombin at 4 ^oC, and APE1 fractions were further purified to homogeneity using HiTrap SP HP column by ion-exchange chromatography using the LCC-500 PLUS (Pharmacia). The final fractions were dialyzed against 20 mM Tris (pH 8.0), 150 mM NaCl, 0.1 mM EDTA, 1 mM DTT, and 50% glycerol, and stored at -20 ^oC.

AP-Endonuclease Activity and EMSA:

A 43-mer oligo nucleotide duplex containing tetrahydrofuran (THF) at position 31 in the sequence 5' ATCTGATTCCCCATCTCCTCAGTTTCACTXCTGCACCGCA TG 3' (X: THF) was purchased from Midland Inc. (USA) and prepared as described previously **[18, 20, 21].** The oligo was 5'-end-labeled with [γ-^{32}P]ATP and T4 polynucleotide kinase (PNKP). After annealing to the complementary strand with C opposite THF, the duplex oligo was purified by gel filtration column (Clontech, Chroma Spin TE 10).

Duplex THF-containing oligo was incubated with recombinant WT APE1 (0.1 nM) at 37 °C (3 min and 30 min) or E96Q mutant (0.1 or 1.0 nM) at 37 °C for 30 min in a 15 µl reaction mixture containing 50 mM Tris–HCl (pH 8), 50 mM KCl, with $MgCl_2$ (2, 5, and 10 mM) or without, 1 mM DTT, 0.1 mM EDTA and 100 µg/ml bovine serum albumin. After stopping the reaction by adding 10 µl 80% formamide/40 mM NaOH containing 0.05% xylene cyanol, followed by heating at 95 ^oC for 5 min and cooling on ice, the samples were analyzed by denaturing gel electrophoresis in 15% polyacrylamide containing 8 M urea to separate the substrate DNA from the cleaved product. Gels were then analyzed with a phosphorescence detection system (Storm, Molecular Dynamics).

The radiolabel THF oligo (about 25 pM) was incubated with 0.1 nM WT or E96Q mutant APE1 in the absence or presence of

Mg^{2+}, and the protein-DNA complexes were analyzed in the EMSA-binding buffer containing 40 mM HEPES, 50 mM KCl, and 1 mM DTT for 15 min at 37 °C followed by electrophoresis in non-denaturing 6% polyacrylamide gel containing 7 mM Tris-HCl (pH 8.0), 3.3 mM sodium acetate and 1 mM EDTA at 4 °C for 1 h at 100 V and the radioactivity in the gels were analyzed as described **[22, 20].**

MD Simulation:

All MD simulations were performed using programs from the AMBER9 suite **[23].** The parameters were NPT ensemble (P = 1 bar and T = 315 K) with periodic boundary conditions and ff03 force field parameters **[24].** We constructed models for the APE1 complexed with AP site-containing oligonucleotide and Mg^{2+} from conformations that we had generated in aforementioned MD simulation study **[14].** In that study, we used a systematic grid search to determine low potential energy binding sites for one Mg^{2+} ion in APE1. These low potential energy sites were clustered at the A and B sites. For the current simulations with Mg^{2+} at the A or B site, we used the same A and B site low potential energy conformations. In the simulations with two Mg^{2+} ions, we started with the A site lowest potential energy conformation and superimposed on this the B site position for the second Mg^{2+}. We generated single E96Q and double ED APE1 mutants by deleting first the side chain oxygen atoms at positions 96 and 210. Then we added the missing oxygen and NH_2 atoms for these positions using the XLEAP module of the AMBER9 package. Same module was also used to add Na^+ ions to achieve electrostatic neutrality. Next, we soaked the complexes in TIP3 water boxes **[25]** large enough to ensure that each box wall was at least 10 Å away from any complex atom.

After constructing the complexes of APE1, its AP site containing 11-mer oligo substrate, cofactor Mg^{2+} and the water box, we first energy-minimized the complexes over 2000 steps and then continued with MD simulation over 1 ns for single Mg^{2+} (A or B site) and 2 ns for two Mg^{2+} (A+B) complexes. Finally, the recorded trajectories were analyzed with PTRAJ from the AMBER package and the snapshots were visualized with the program MOLMOL **[26].**

Results:

WT and E96Q Mutant APE1 polypeptides have endonuclease activity in the presence of Mg^{2+}:

WT APE1 and the E96Q mutant proteins purified to near homogeneity **(Figure 1a)** were tested for Mg^{2+} at the active site by measuring AP endonuclease activity. We used a 43-mer duplex oligo containing THF at position 31 in the standard assay buffer containing 2 mM Mg^{2+} as described in the Methods. While no activity was observed with 0.1 nM E96Q mutant, increasing the concentration by 10 times (1.0 nM) in the presence of 2 mM Mg^{2+} cleaved the substrate after 30 min incubation **(Figure 1b).** Such Mg^{2+}-dependent cleavage activity in the E96Q mutant was confirmed using two independent preparations of the mutant protein. We therefore concluded that the E96Q APE1 mutant is indeed capable of binding Mg^{2+}. Both WT and E96Q mutant APE1 were able to bind the THF oligo in the absence of Mg^{2+}. Addition of Mg^{2+} activated the WT enzyme resulting in the loss of the oligo bound APE1 complex. In contrast, the E96Q mutant APE1 remained bound to the THF oligo **(Figure 1c)** presumably because of its slow turnover **(Figure 1b).** These results are consistent with previous results **[20, 27, 13, 28]** which showed that the E96 mutants had less activity than the WT enzyme but retained Mg^{2+}-dependence for its activity. The highest endonuclease activity for the E96Q mutant was observed at 5 mM Mg^{2+} **(Figure 1b**) which was comparable to 8 mM Mg^{2+} needed for optimum activity of the E96A mutant we had observed earlier. Also, consistent with the previous study, higher Mg^{2+} concentration inhibited AP site-cleavage activity **[27].**

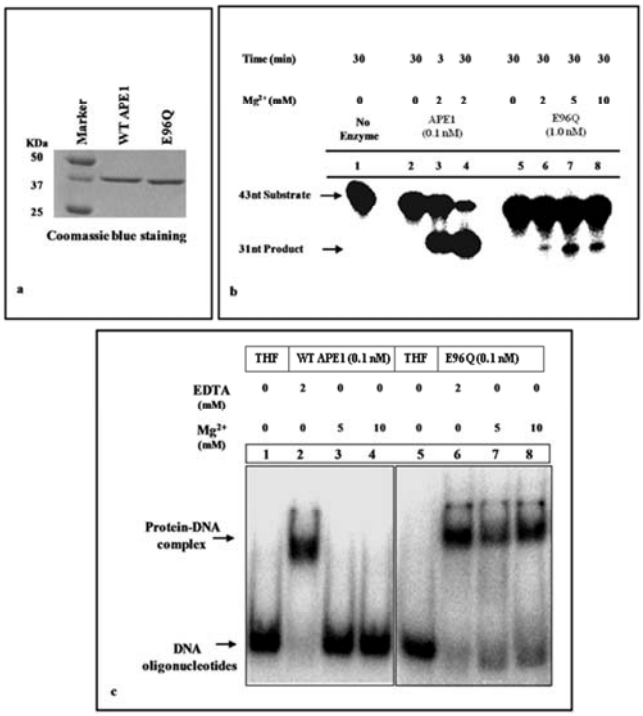

Figure 1: **a)** Coomassie blue staining of purified WT and E96Q mutant APE1 proteins (0.5 µg protein) after SDS-PAGE (10% polyacrylamide); lane 1, marker; lane 2, WT APE1; and lane 3, E96Q proteins. **b)** AP-endonuclease activity was measured using 43-mer, THF- containing oligonucleotide. WT APE1 (0.1 nM) was incubated for 3 min at 37 °C as shown in lanes 2, 3, and 4 using a buffer containing 50 mM Tris-HCl (pH 8.0), 50 mM KCl and in absence or in presence of 2 mM Mg^{2+} respectively. The endonuclease activity of E96Q (1.0 nM) mutant APE1 was measured in the absence or in presence of 2, 5, and 10 mM Mg^{2+} as shown in lanes 5, 6, 7, and 8 respectively for 30 min at 37 °C. **c)** EMSA of THF-DNA binding by WT and E96Q (0.1 nM) mutant APE1 proteins. Lane 1, no protein; lane 2, WT APE1 without Mg^{2+}; lanes 3 & 4, with 5 and 10 mM Mg^{2+} respectively; lane 5, no protein; lane 6, E96Q without Mg^{2+}; lanes 7 & 8, with 5 and 10 mM Mg^{2+} respectively. While lanes, 2 & 6 supplemented with 2 mM EDTA. The data represent three or more independent experiments.

Mg^{2+} bound at the A site destabilizes substrate DNA:

In all three simulations of WT, E96Q and ED APE1 with the Mg^{2+} bound at the A site, the substrate DNA shifted significantly from its starting position **(Figure 2 and S2).** Placing a Mg^{2+} at the A site interfered with the H-bond chain D283-H309-AP phosphate oxygen (yellow dotted line in **Figures 2-6 and S2-S6**), preventing the H-bond between H309 and the AP phosphate oxygen that is essential for substrate binding and

cleavage, as indicated by 13 fold higher Km of the H309N mutant than of WT enzyme **[29, 30].**

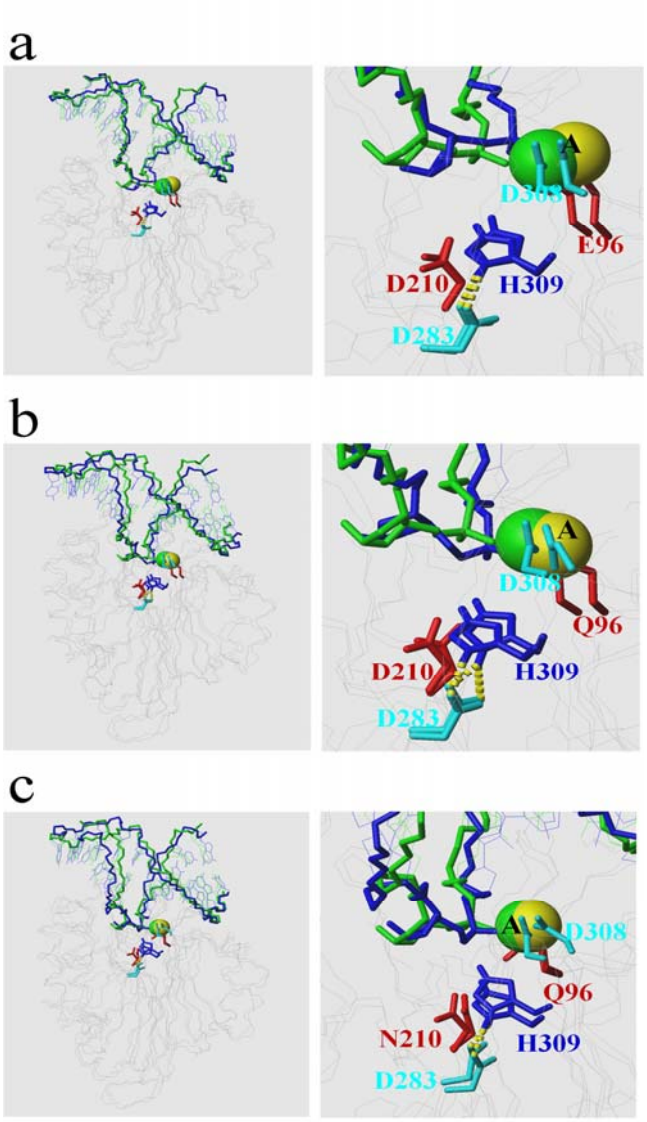

Figure 2: Snapshots of the A site MD-simulations after initial minimization (green) and after 1 ns simulation (blue). Panels on the left and right show global and closeup views. WT, E96Q and ED snapshots are shown in a, b and c.

The final substrate DNA binding site was different for each complex in these simulations with Mg^{2+} at the A site (**Figure 5a and S5a**). In agreement with the crystal structure of the product-APE1- Mg^{2+} complex (PDB-code 1DE9), Mg^{2+} in the pre-cleavage DNA-APE1- Mg^{2+} complex was coordinated by E/Q96 side chains. In WT APE1 simulation, Mg^{2+} was hexagonally coordinated by both E96 side chain oxygens, one oxygen each from D308, D70, AP phosphate and a water molecule. The residues D308 and D70 are among the conserved residues in APE1 and related sequences **[31,32].** Similarly, in E96Q and ED mutant simulations, Mg^{2+} was coordinated by both side chain oxygens of D308, and one oxygen each of Q96 (instead of E96), D70, AP phosphate and a water molecule. However, in the 1 ns WT simulation, the AP site P-atom position was 4.1 Å away from its crystal structure (1DE9) position with the product and Mg^{2+} ion **(Table 2, see supplementary material).** This distance between the crystal structure of the substrate-DNA complex (1DE8) and the WT simulation was even larger (4.8 Å). Same distance of the AP site P-atoms between the two crystal structures **[8]** (1DE9 and 1DE8) is 1.0 Å. In agreement with this we showed in a previous study **[20],** that Mg^{2+} bound at the B site had pulled the substrate DNA by 1.0 Å toward D210.

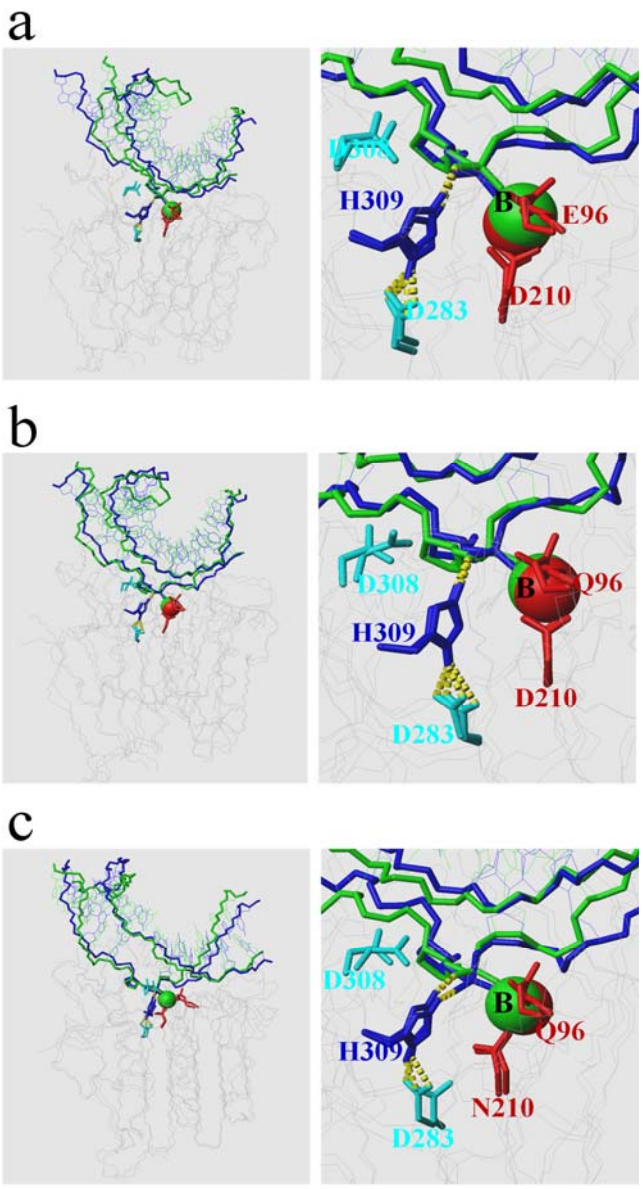

Figure 3: Snapshots of the B site MD-simulations after initial minimization (green) and after 1 ns simulation (blue). Panels on the left and right show global and closeup views. WT, E96Q and ED snapshots are shown in a, b and c.

Mg^{2+} ion at the B site leaves the pre-cleavage substrate DNA close to the position observed in the crystal structure:
Unlike for the A site simulations, placing the Mg^{2+} at the B site left the substrate DNA close to its starting crystal structure

position (1DE8). In the simulations of WT, E96Q and ED proteins, the B site Mg^{2+} did not shift the AP site **(Figure 3 and S3),** and the final position of the AP site in all three simulations were very close to one another **(Figure 5b and S5b).** The H-bond chain D283-H309-AP site phosphate oxygen was intact in all three simulations **(Figure 3, 6 and S3,S6).** Furthermore, in contrast to the A site simulations, placing the Mg^{2+} at the B site kept the AP site P-atom close to the corresponding crystal structure P-atoms in the product plus Mn^{2+} (1DE9) and substrate (1DE8) containing crystal structures (0.9 Å and 1.8 Å).

The B site Mg^{2+}, contrary to the assumption of Lipton *et al.* **[17]** and others that E96 is only a A site ligand and therefore would coordinate only the A site metal ion, was coordinated also by the E/Q96 side chains. Similar behavior we had observed in earlier simulations **[20,14].** We always found that the E96 side chain coordinated the Mg^{2+} ion, and followed the movement of the Mg^{2+} ion from the B to the A site. During the migration of the Mg^{2+} from the B to the A site the OE2 atom on E96 needed to move only 2.07 Å. **Figures 6 and S6a** show the active site and coordination of the B site Mg^{2+} after 1 ns WT simulation. Here and in the other two B site simulations the Mg^{2+} was hexagonally coordinated by the side chains of E96, N212, D210 (both side chain oxygens), AP phosphate oxygen and a water molecule.

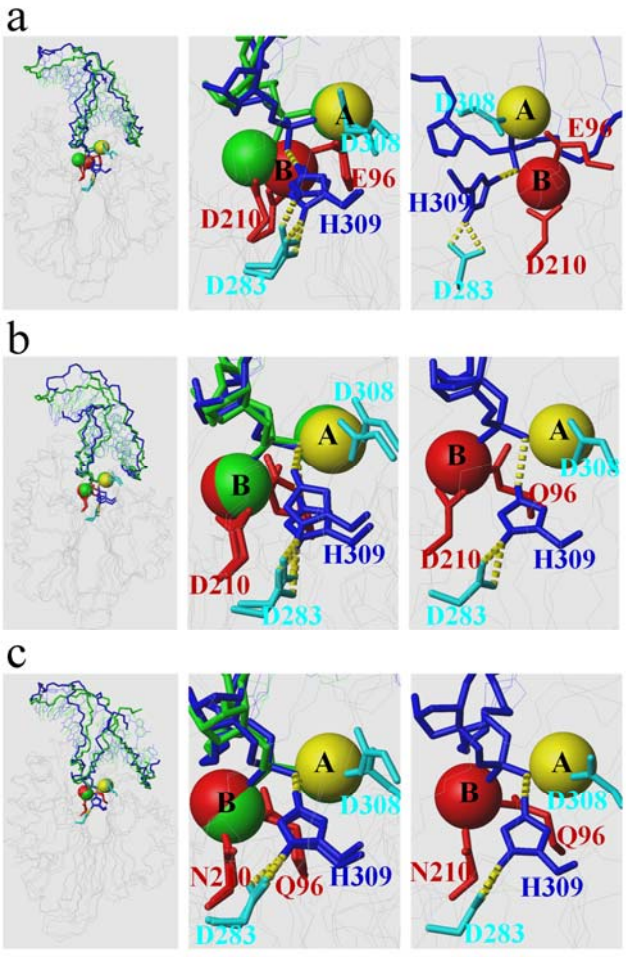

Figure 4: Snapshots of the A+B site MD-simulations after initial minimization (green) and after 2 ns simulation (blue). Panels on the left and right show global and closeup views. WT, E96Q and ED snapshots are shown in a, b and c.

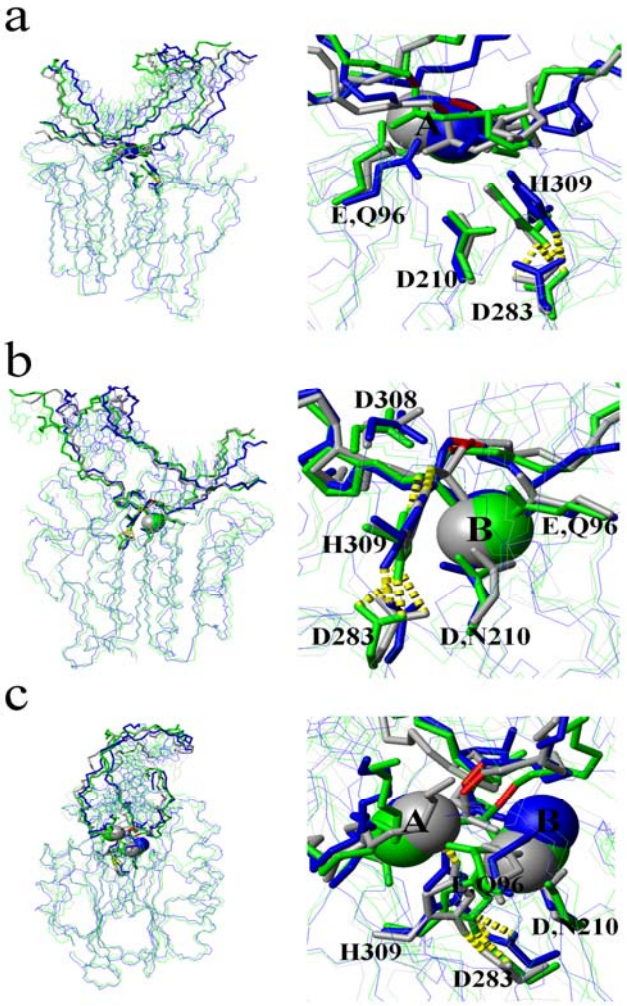

Figure 5: Superposition of the final snapshots of the WT (green), E96Q (grey) and ED simulations (blue). On the left and right are global and closeup views shown. The simulations with one Mg^{2+} (A and B site) were run over 1 ns, while the simulations with two Mg^{2+} (A+B) were run over 2 ns.

AP phosphate oxygens bridge A and B site bound Mg^{2+} ions

In the MD-simulations with two Mg^{2+} ions bound at the A and B site, the Mg^{2+} ions were bridged by the AP site phosphate oxygens. Additionally, E96 in the WT simulation also bridged the two Mg^{2+} ions (**Figures 4, 5c and S4, S5c**). This behavior was different from what we observed in earlier simulations **[14]** where we started with two Mg^{2+} ions at the Pb^{2+}position in APE1's crystal structure 1E9N **[10].** In the current simulations, we started with two grid search positions (low potential energy positions) **[14].** Earlier, the two Mg^{2+} ions moved away from each other **[14],** while in these simulations they moved closer. They were stabilized by phosphate oxygens of the AP site and additionally by the E96 carboxyl group in WT APE1 simulation **(Figure S6b).** In the E96Q and ED APE1 simulations, the side chain oxygen of Q96 coordinated only the B site Mg^{2+} and could

not bridge both Mg^{2+} ions. Nevertheless, the H-bond chain D283-H309-AP site phosphate oxygen was intact (yellow dotted lines in **Figures 4, 5c and S4, S5c, S6b).** The distances between the AP site P-atom positions from the WT simulation with two Mg^{2+} (at sites A+B) to the corresponding P-atom positions in the crystal structures (1DE8: substrate alone and 1DE9: product plus Mn^{2+}) were 2.1 Å and 1.2 Å. These distances were larger than the distances from the WT APE1 simulation with one Mg^{2+} ion bound at the B site to the same crystal structures (1.8 Å and 0.9 Å) **(Table 2, see supplementary material).**

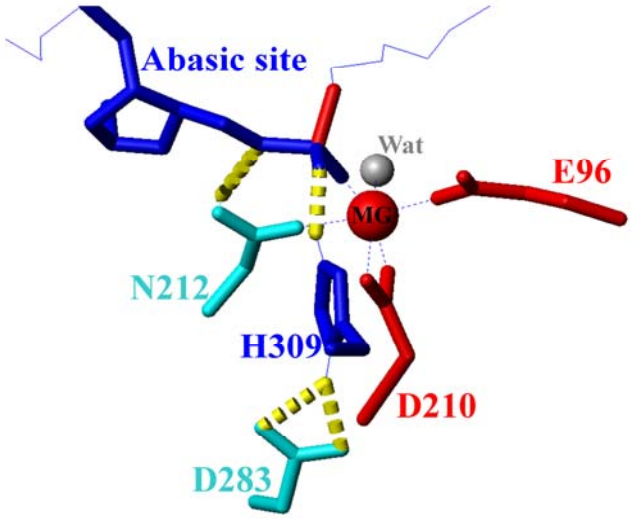

Figure 6: Active site and Mg^{2+} coordination at the end of the 1 ns WT simulation with AP containing DNA substrate and Mg^{2+} at the B site.

Discussion:

As noted in the introduction, the exact stoichiometry of the metal ion in the APE1 cleavage reaction is still being debated because that could only be inferred from indirect measurements. The most reliable way to determine the location of Mg^{2+} during catalysis is by analysis of the active site of crystal structures **[8-11].** As we previously discussed, such data for APE1 indicate two different binding sites for Mg^{2+} (A and B site). Although solid-state ^{25}Mg NMR has been proposed as a way to quantitate the number of metal ions bound, this method is still problematic, because of background due to nonspecific Mg^{2+} binding. While Lipton *et al.* **[17]** identified, in the first part of their study, two different Mg^{2+} signals originating from Mg^{2+} bound in the active site of free APE1 (no substrate-bound), they could not establish the positions for these two Mg^{2+} ions. Our previously described grid search data indicated that there were two, low potential energy positions for Mg^{2+} ions. These were close to the positions of metal ions in the crystal structures **[14].** In our current MD-simulations with two Mg^{2+} ions at the A and B site the APE1-substrate-Mg^{2+} ions complex was also stable. Therefore, the two different Mg^{2+} signals from the solid state NMR study are consistent with both (1DE8 and 1DE9) crystal structures, our "moving metal" model and the two Mg^{2+} complex presented in this study. However, the rejection of the B site in the second part of the solid state NMR study **[17]** Lipton *et al.* is not justified. Logical consequence of the argumentation of Lipton *et al.* would be that neither the ED nor E96Q mutant would be able to bind any Mg^{2+} at the active site. In this study we showed qualitative experimental confirmation of earlier results from Erzberger *et al.* **[13],** Nguyen *et al.* **[33]** and Chou *et al.* **[28],** that the E96Q mutant has Mg^{2+}-dependent (low but detectable) endonuclease activity. Although these experiments did not allow the determination of the specific location of the Mg^{2+} (A or B site) on APE1, it is safe to conclude that Mg^{2+} was bound at the active site. In MD simulations for this study we showed that Mg^{2+} binding at the A site alone is very unlikely. Assuming that the ion does not move, this Mg^{2+} position would be consistent with the crystal structure of the APE1-cleaved DNA-Mn^{2+} complex (1DE9). However, the distance between the Mn^{2+} and D210 in this crystal structure is larger than 5.5 Å. Therefore, this crystal structure cannot explain the complete loss of endonuclease activity in D210 mutants **[12, 13].** This is also the weakness of the one Mg^{2+} mechanism that shows the Mg^{2+} bound at the A site **[8].** Additionally, placing only one Mg^{2+} at the A site destabilized the substrate in the MD simulations. It also interfered with the H-bond chain D283-H309-AP site, which is critical for substrate binding **[29, 30].** Placing the Mg^{2+} at the B site on the other hand kept the substrate DNA stable at its crystal structure position and the H-bond chain D283-H309-AP site phosphate intact. The B site Mg^{2+} was coordinated by D210, which explains the essential role of D210 for the endonuclease activity. Further, B site Mg^{2+} shifted the AP site of the substrate closer to D210 and closer to the AP site position in the crystal structure with the product (1DE9). Assuming that Mg^{2+} is bound at the B site prior to cleavage, it has to move to the A site after cleavage in order to be consistent with the APE1-product-Mn^{2+} crystal structure (1DE9). This is essentially our "moving metal" mechanism **[14]** based on MD simulations. As shown in **Figure 6 and S6a**, the B site Mg^{2+} was coordinated pre-cleavage by E96, D210, N212, AP-phosphate and a water molecule. In our mechanism D210 accepts the proton during the activation process of the Mg^{2+} bound water molecule to create the nucleophile OH-. In that process the acquired proton weakens the D210-Mg^{2+} interaction and repels the Mg^{2+} that then moves to the A site. N212 has been shown to be involved in substrate binding **[34],** which could also be explained in our model. N212 coordinated the Mg^{2+} and forms a H-bond with the substrate. E96 is located between the A and B site enabling it to coordinate the Mg^{2+} at both sites. In all simulations we observed that it was coordinating a Mg^{2+} independent of where the Mg^{2+} was located. In our current MD-simulations with two Mg^{2+} ions at the A+B site the important H-bond chain D283-H309-AP site also remained intact. The AP site phosphate oxygens and the E96 side chain oxygens bridged the Mg^{2+} ions **(Figure S6b)** and left the substrate relatively stable. However, the AP site positions in the single B site Mg^{2+} simulations were closer to the crystal structure positions (1DE8 and 1DE9) than the AP site position in the simulations with two Mg^{2+} ions at the A+B sites. Additionally, in the crystal structure with the product bound (1DE9), there is only one Mn^{2+} ion. In our MD-simulations we started with conformations close to the global minimum, namely the crystal structure 1DE8. Therefore, in general one would expect small conformational changes that represent only local rearrangements and fluctuations around this minimum. We saw this kind of fluctuations with the B and A+B site simulations. The A site simulation on the other hand showed even at the end of our relatively short simulation time large changes compared with the initial conformation. This indicates

that placing one Mg^{2+} ion at A site did change the energy landscape drastically. Accordingly, longer simulation would show only even larger conformational changes. Finally, we predict that solving the crystallographic structure of Mg^{2+} bound to the D210N mutant will unequivocally establish the pre-cleavage position and number of Mg^{2+} ion(s). Because the D210N mutation renders APE1 totally inactive, the Mg^{2+} ion(s) would be trapped in their pre-cleavage position(s), which should be evident in the protein structure.

Acknowledgement:
This research was supported by USPHS grants RO1 CA53791 and P30 ES006676 (to S.M.) and US DOE grant DE-FG02-04ER63826 (to W.E.B.). We thank Dr M. Hegde at the University of Texas Medical Branch (UTMB) for helpful discussions during the study. We also thank Dr. T. Wood of the Recombinant DNA Laboratory for DNA sequencing.

References:

[1] Marnett LJ & Burcham PC, *Chem Res Toxicol.* 1993 **6:** 771 [PMID:8117915]
[2] Barnes DE & Lindahl T, *Annu Rev Genet.* 2004 **38:** 445 [PMID:15568983]
[3] Doetsch PW & Cunningham RP. *Mutat Res.* 1990 **236:** 173 [PMID:1697933]
[4] Demple B & Harrison L, *Annu Rev Biochem.* 1994 **63:** 915 [PMID:7979257].
[5] Wilson SH. *Mutat Res.* 1998 **407:** 203 [PMID:9653447]
[6] Evans AR *et al. Mutat Re134s.* 2000 **461:** 83 [PMID:11018583]
[7] Mundle ST *et al. Biochemistry* 2009 **48:** 19 [PMID:2731572]
[8] Mol CD *et al. Nature* 2000 **403:** 451 [PMID:10667800]
[9] Gorman MA *et al. EMBO J.* 1997 **16:** 6548 [PMID:1170259]
[10] Beernink PT *et al. J Mol Biol.* 2001 **307:** 1023 [PMID:11286553]
[11] Georgiadis MM *et al. Mutat Res.* 2008 **643:** 54 [PMID:2637456]
[12] Rothwell DG *et al. Nucleic Acids Res.* 2000 **28:** 2207 [PMID:102632]
[13] Erzberger JP & Wilson DM, *J Mol Biol.* 1999 **290:** 447 [PMID:10390343]
[14] Oezguen N *et al. Proteins* 2007 **68:** 313 [PMID:17427952]
[15] Kashiwagi T *et al. Protein Eng.* 1996 **9:** 857 [PMID:8931125]
[16] Pingoud V *et al. J Mol Biol.* 2009 **393:** 140 [PMID:19682999]
[17] Lipton AS *et al. J Am Chem Soc.* 2008 **130:** 9332 [PMID:2564828]
[18] Izumi T *et al. J Mol Biol.* 1999 **287:**47 [PMID:10074406]
[19] Izumi T & Mitra S, *Carcinogenesis* 1998 **19:**525 [PMID:9525290]
[20] Mantha AK *et al. J Mol Biol.* 2008 **379:** 28 [PMID:2708089]
[21] Ramana CV *et al. Proc Natl Acad Sci U S A.* 1998 **95:** 5061 [PMID:20213]
[22] Izumi T *et al. Biochemistry* 2004 **43:** 684 [PMID:14730972]
[23] Case DA *et al. J Comput Chem.* 2005 **26:** 1668 [PMID:1989667]
[24] Ponder JW & Case DA, *Adv Protein Chem.* 2003 **66:** 27 [PMID:14631816]
[25] Jorgensen WL *et al. J Chem Phys.* 1983 **79:** 926 [DOI:10.1063/1.445869]
[26] Koradi R *et al. J Mol Graph.* 1996 **14:** 51 [PMID:8744573]
[27] Barzilay G *et al. Nat Struct Biol.* 1995 **2:** 561 [PMID:7664124]
[28] Chou KM & Cheng YC, *J Biol Chem.* 2003 **278:** 18289 [PMID:12624104]
[29] Masuda Y *et al. J Biol Chem.* 1998 **273:** 30360 [PMID:9804799]
[30] Lucas JA *et al. Biochemistry* 1999 **38:** 4958 [PMID:10213597]
[31] Schein CH *et al. BMC Bioinformatics* 2002 **3:** 37 [PMID:149231]
[32] Schein CH *et al. Proteins* 2005 **58:** 200 [PMID:15505785]
[33] Nguyen LH *et al. J Mol Biol.* 2000 **298:** 447 [PMID:8117915]
[34] Rothwell DG & Hickson ID, *Nucleic Acids Res.* 1996 **24:** 4217 [PMID:146231]

Edited by VS Mathura
Citation: Oezguen *et al.* Bioinformation 7(4): 184-198 (2011)

BIOINFORMATION

open access

Supplementary material:

Table 1: Crystal structures of APE1

PDB-code	Resolution	Metal ions	Substrate/Product DNA
1DE8[a]	2.9Å	---	Not cleaved substrate with one AP site (11 bp)
1DEW[a]	2.7Å	---	Not cleaved substrate with one AP site (15 bp)
1DE9[a]	3.0Å	Mn^{2+} (at the active site)	Cleaved product 5′ to the AP site (9 bp)
1BIX[b]	2.2Å	4 Sm^{3+}, 1 Pt^{2+} (one Sm^{3+} at the active site)	---
1HD7[c]	2.0Å	Pb^{2+} (at the active site)	---
1E9N[c]	2.2Å	2 Pb^{2+} (both at the active site)	---
2O3H[d]	1.9Å	2 Sm^{3+} (one at the active site)	---
2O3C[d]	2.3 Å	3 Pb^{2+} (one at the active site)	---
2ISI[e]	2.8 Å	1 Mg^{2+} (at the active site)	---

[a]Mol *et al.* 2000 **[8]**
[b]Gorman *et al.* 1997 **[9]**
[c]Beernink *et al.* 2001 **[10]**
[d]Georgiadis *et al.* 2008 **[11]**
[e]Reference not available

Table 2: Effect of the Mg^{2+} position on the AP site P-atom distances (Å)

		WT APE1 MD-simulations			Crystal Structures	
		A	**B**	**A+B**	**1DE8**	**1DE9 (A)**
WT APE1 MD-simulations	**A**	---	4.1	4.0	**4.8**	**4.1**
	B	4.1	---	0.7	**1.8**	**0.9**
	A+B	4.0	0.7	---	**2.1**	**1.2**
Crystal Structures	**1DE8**	4.8	1.8	2.1	---	**1.0**
	1DE9 (A)	4.1	0.9	1.2	1.0	---

Supplementary figures:

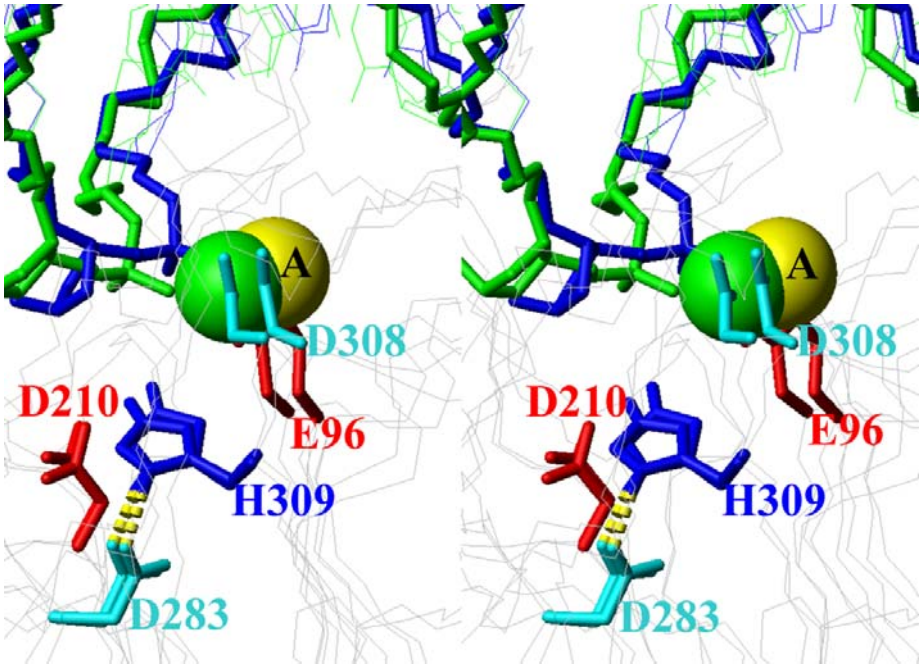

Figure S2a: Stereo view of the snapshots of the WT A site MD-simulationafter initial minimization (green) and after 1 ns simulation (blue).

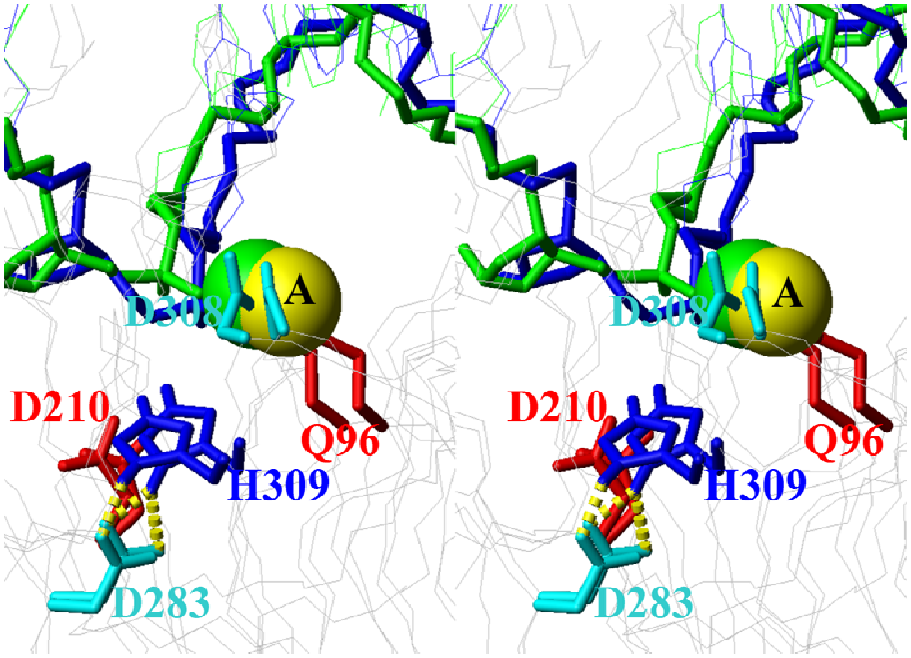

Figure S2b: Stereo view of the snapshots of the E96Q mutant Asite MD-simulationafter initial minimization (green) and after 1 ns simulation (blue).

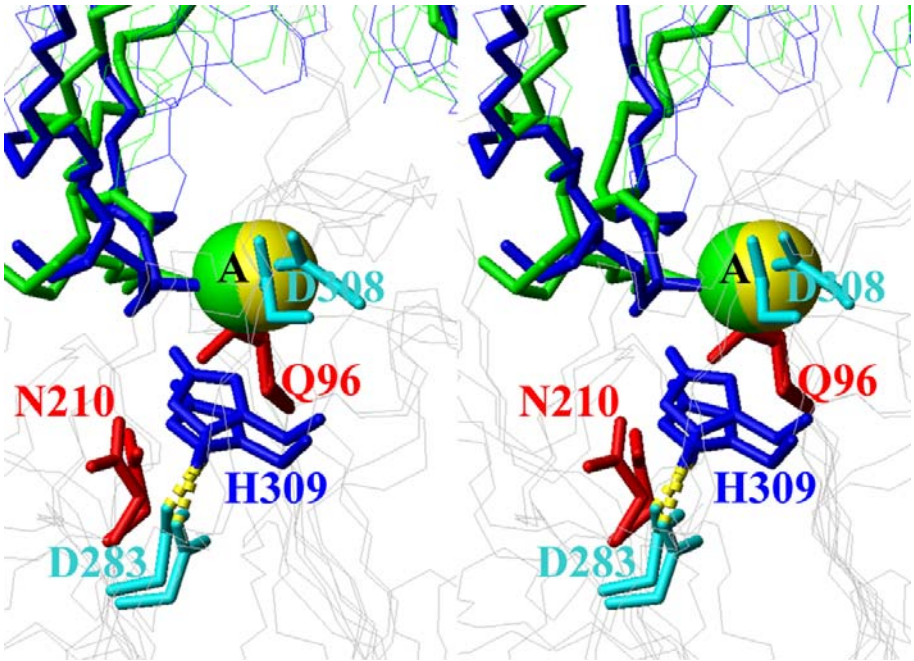

Figure S2c: Stereo view of the snapshots of the ED mutant A site MD-simulationafter initial minimization (green) and after 1 ns simulation (blue).

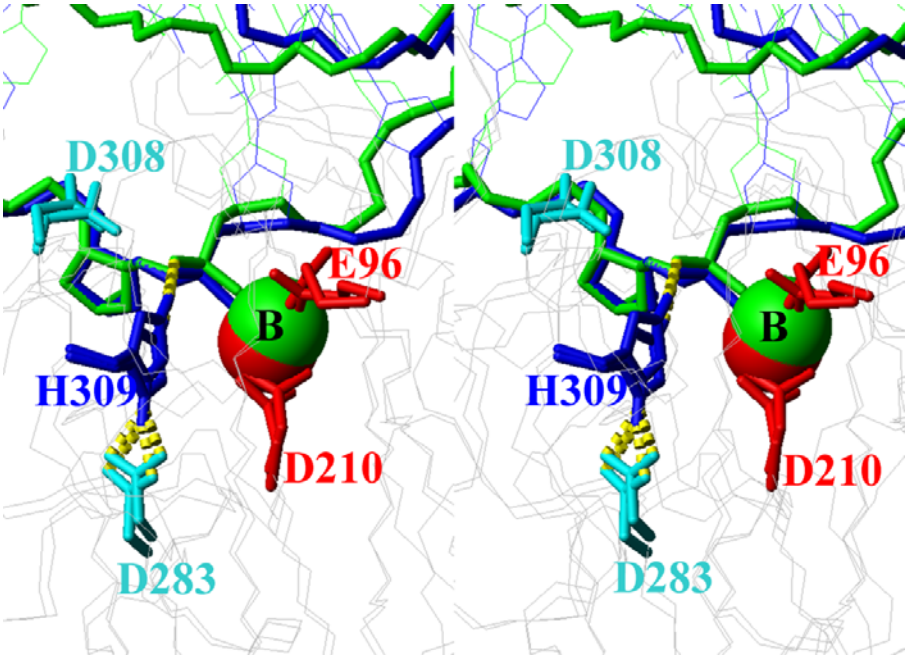

Figure S3a: Stereo view of the snapshots of the WT B site MD-simulationafter initial minimization (green) and after 1 ns simulation (blue).

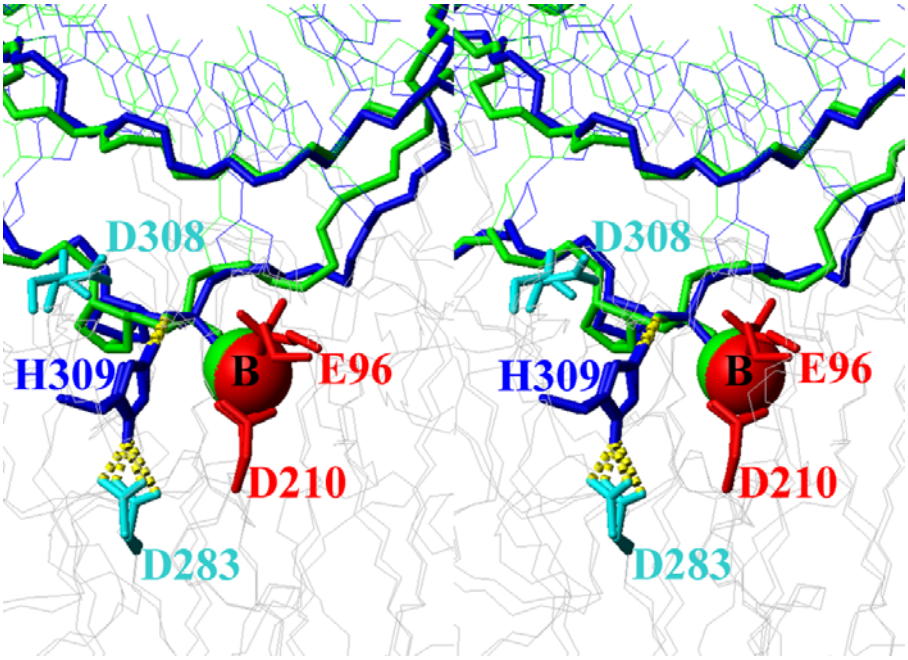

Figure S3b: Stereo view of the snapshots of the E96Q mutant B site MD-simulationafter initial minimization (green) and after 1 ns simulation (blue).

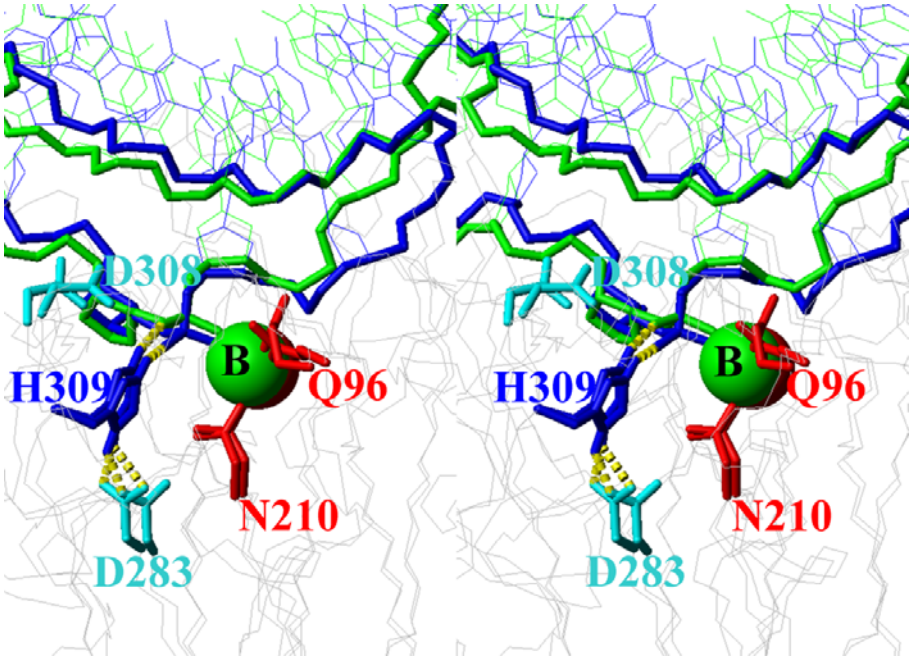

Figure S3c: Stereo view of the snapshots of the ED mutant B site MD-simulationafter initial minimization (green) and after 1 ns simulation (blue).

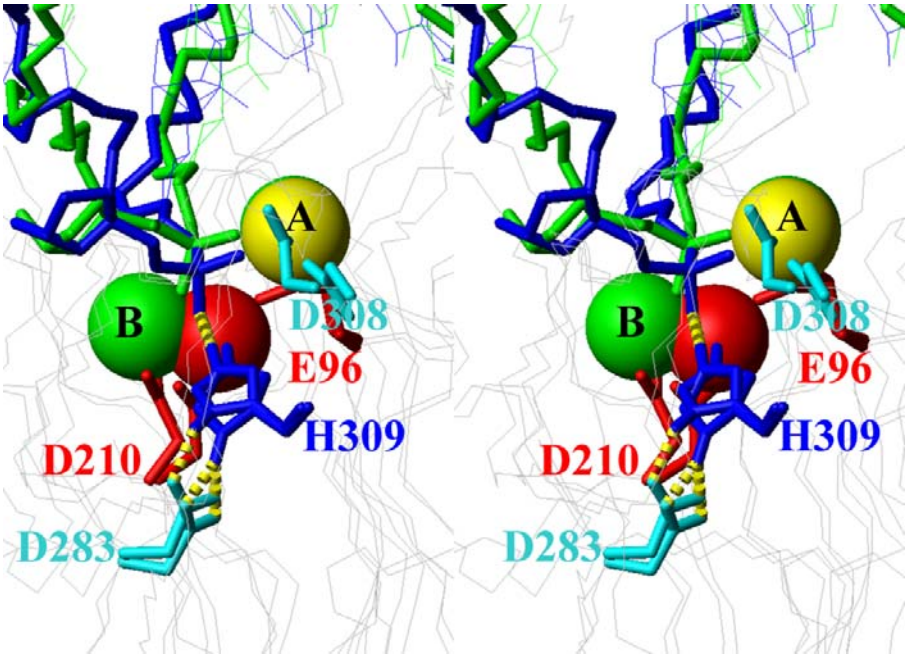

Figure S4a: Stereo view of the snapshots of the WT AB site MD-simulationafter initial minimization (green) and after 1 ns simulation (blue).

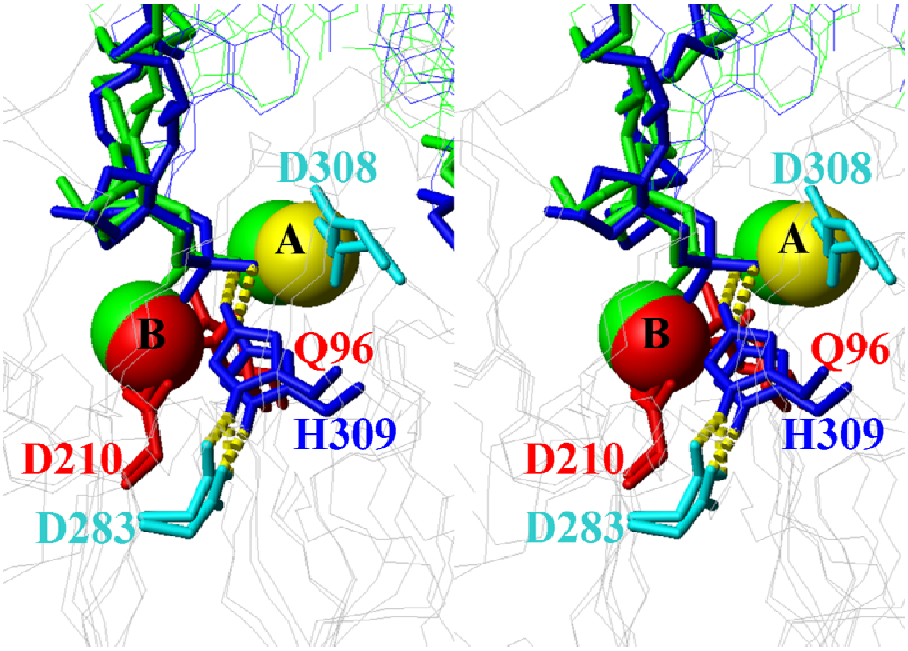

Figure S4b: Stereo view of the snapshots of the E96Q mutant AB site MD-simulationafter initial minimization (green) and after 1 ns simulation (blue).

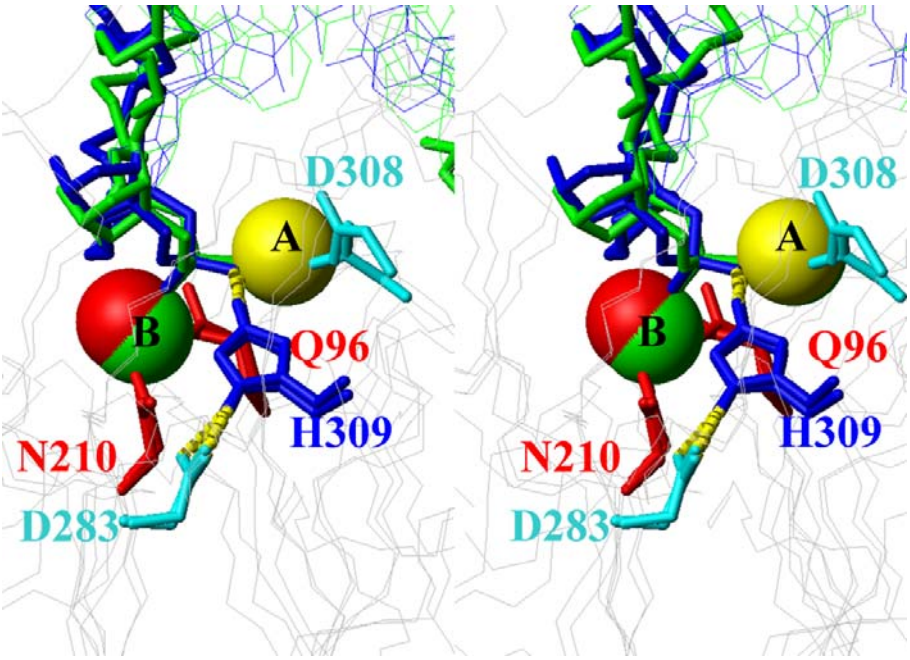

Figure S4c: Stereo view of the snapshots of the ED mutant AB site MD-simulationafter initial minimization (green) and after 1 ns simulation (blue).

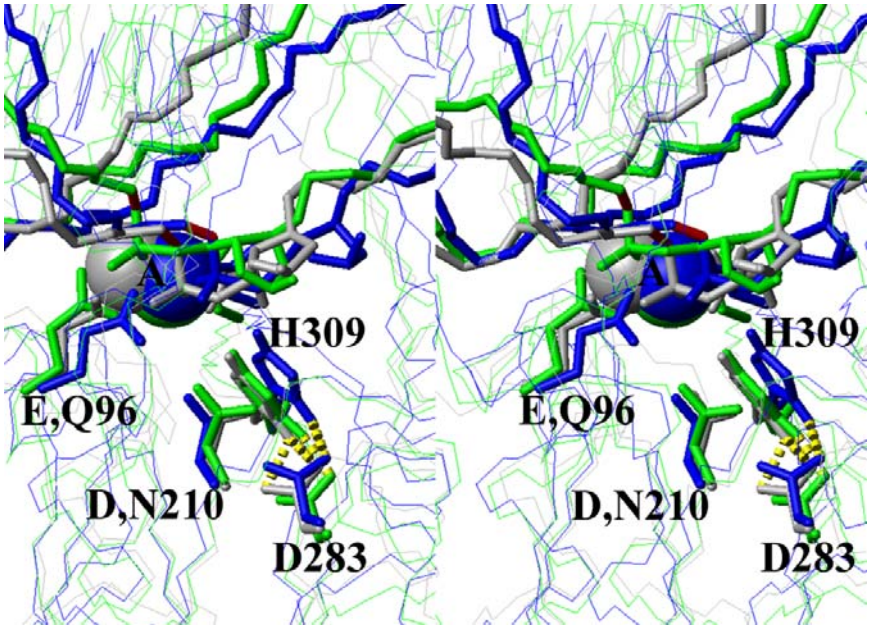

Figure S5a: Superposition of the 1 nssnapshots of the A site simulations of WT (green), E96Q (grey) and ED simulations (blue).

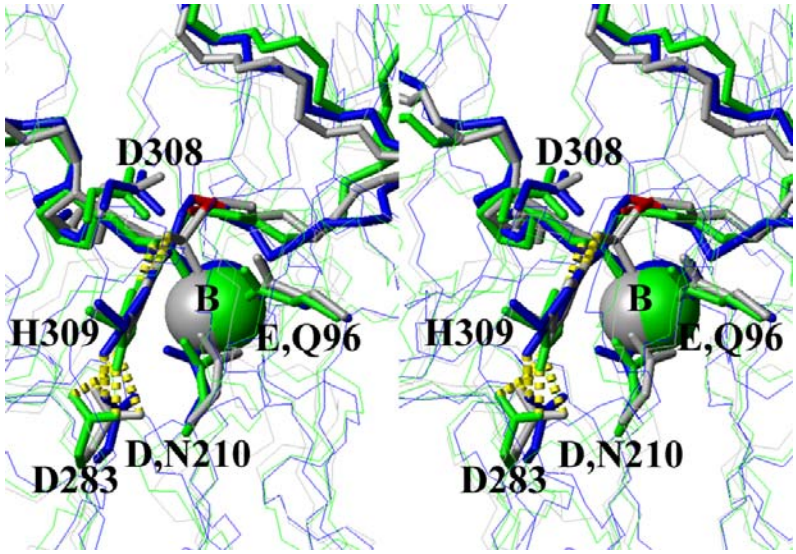

Figure S5b: Superposition of the 1nssnapshots of the B site simulations of WT (green), E96Q (grey) and ED simulations (blue).

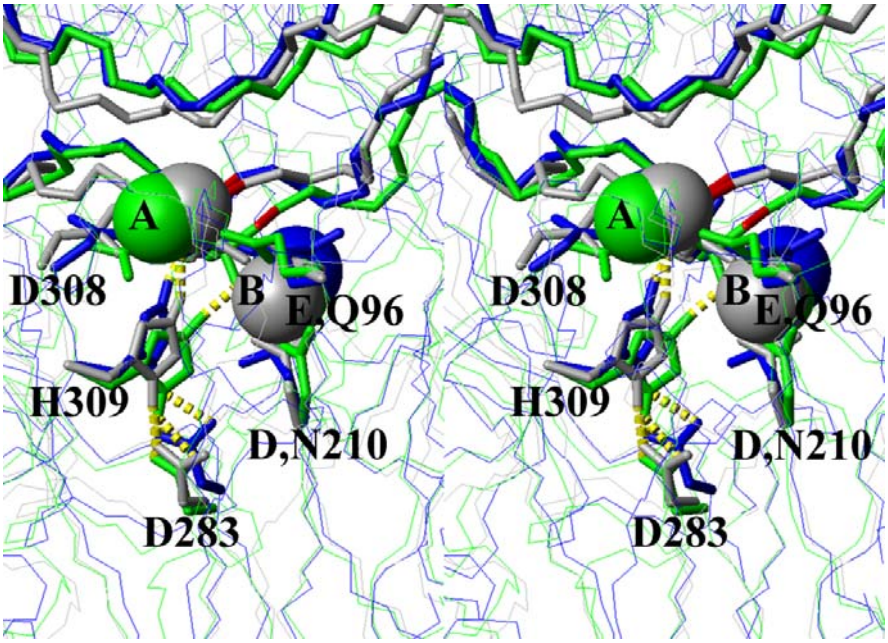

Figure S5c: Superposition of the 2 ns snapshots of the A+B site simulations of WT (green), E96Q (grey) and ED simulations (blue).

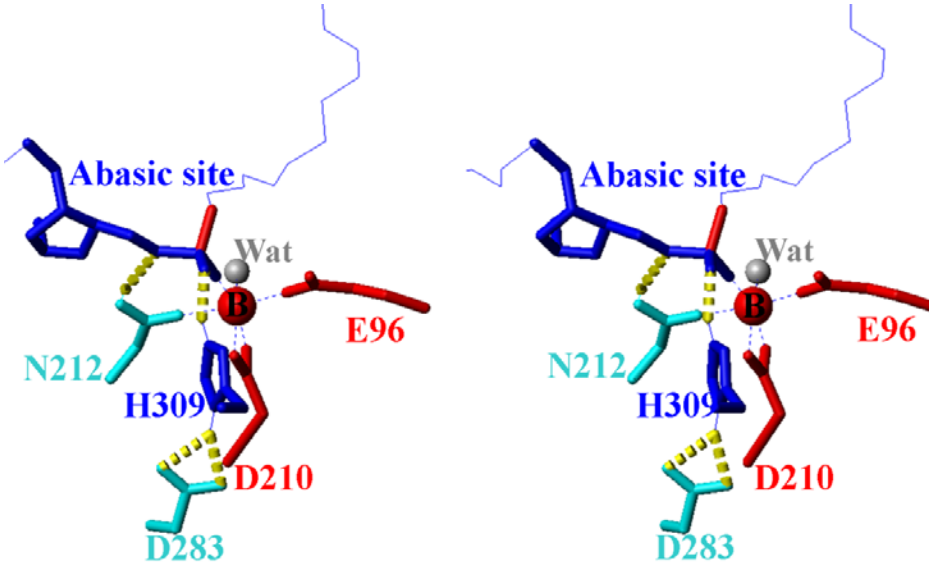

Figure S6a:Stereoview of the active site and Mg^{2+} coordination at the end of the 1 ns WT simulation with AP containing DNA substrate and Mg^{2+}at the B site.

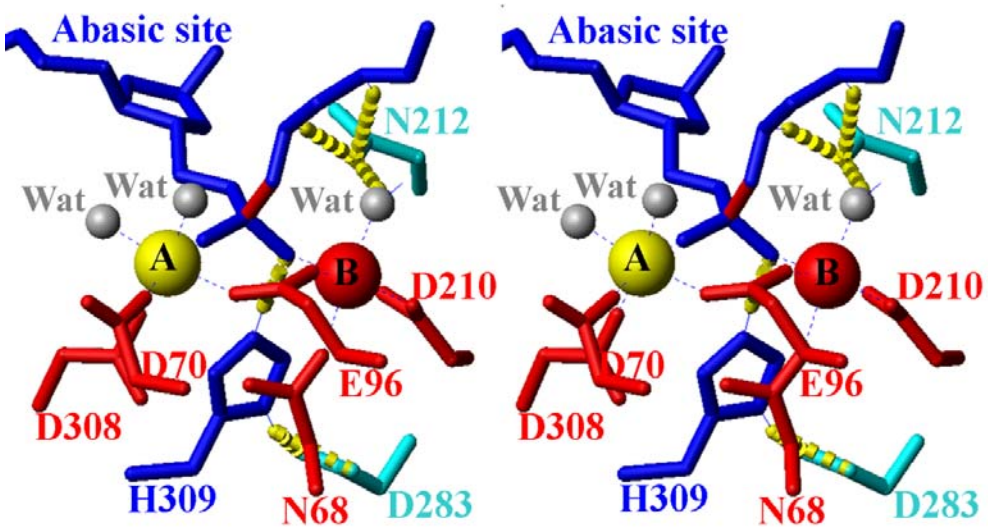

Figure S6b:Stereoview of the active site and the 2 Mg^{2+}ions coordination at the end of the 2 ns WT simulation with AP containing DNA substrate and 2 Mg^{2+}ions at the A+B site.